Crystal field, Dzyaloshinsky-Moriya interaction, and orbital order in La0.95Sr0.05MnO3 probed by ESR

Joachim Deisenhofer, Mikhail V. Eremin, D. V. Zakharov, V. A. Ivanshin, R. M. Eremina, Hans-Albrecht Krug von Nidda, A. A. Mukhin, A. M. Balbashov, Alois Loidl

Crystal field, Dzyaloshinsky-Moriya interaction, and orbital order in La$_{0.95}$Sr$_{0.05}$MnO$_3$ probed by ESR

J. Deisenhofer,[1] M. V. Eremin,[1,2] D. V. Zakharov,[2] V. A. Ivanshin,[1,2] R. M. Eremina,[1,3] H.-A. Krug von Nidda,[1]
A. A. Mukhin,[4] A. M. Balbashov,[5] and A. Loidl[1]

[1]*Experimentalphysik V, EKM, Universität Augsburg, 86135 Augsburg, Germany*
[2]*Kazan State University, 420008 Kazan, Russia*
[3]*E. K. Zavoisky Physical-Technical Institute, 420029 Kazan, Russia*
[4]*Institut of General Physics, Russian Academy of Sciences, 117942 Moscow, Russia*
[5]*Moscow Power Engineering Institute, 105835 Moscow, Russia*

We present a comprehensive analysis of the Dzyaloshinsky-Moriya interaction and crystal-field parameters using the angular dependence of the paramagnetic-resonance shift and linewidth in single crystals of La$_{0.95}$Sr$_{0.05}$MnO$_3$ within the orthorhombic Jahn-Teller distorted phase. The Dzyaloshinsky-Moriya interaction (~ 1 K) results from the tilting of the MnO$_6$ octahedra against each other. The crystal-field parameters D and E are found to be of comparable magnitude (~ 1 K) with $D \approx -E$. This indicates a strong mixing of the $|3z^2-r^2\rangle$ and $|x^2-y^2\rangle$ states for the real orbital order.

I. INTRODUCTION

The importance of orbital degrees of freedom in understanding the complex phase diagrams of manganites[1] is a subject of intense research activities (see, e.g., Refs. 2–4 for an overview). The antiferromagnetic insulator LaMnO$_3$ ($T_N = 140$ K) is an orbitally ordered system,[5] which has been established experimentally by resonant x-ray scattering[6] and neutron diffraction.[7] Moreover, Saitoh *et al.* recently reported evidence for orbital excitations by Raman spectroscopy.[8] The orbital order in LaMnO$_3$ is induced by the cooperative Jahn-Teller (JT) effect of the Mn^{3+} ions (electronic configuration 3d^4: $t_{2g}^3 e_g^1$, spin $S=2$), which at temperatures $T < T_{JT} = 750$ K leads to a strong orthorhombic distortion of the perovskite structure. In the paramagnetic state, electron-spin resonance (ESR) reveals a single exchange-narrowed resonance line with a g value near 2.0 due to all Mn^{3+} ions[9] and hence directly probes the spin of interest. Doping divalent ions such as Sr or Ca as substituents for La^{3+} gradually suppresses the JT distortion and leads to a ferromagnetic insulating and finally to a metallic phase at approximately 15% Sr doping.

In a previous work, we presented a systematic ESR study in single crystals of La$_{1-x}$Sr$_x$MnO$_3$ with Sr concentrations $0 \leq x \leq 0.2$.[10] In the JT distorted phase the resonance linewidth ΔH is strongly enhanced compared to the undistorted phase, reaching maximum values of about $\Delta H_{max} \approx 2.5$ kOe. Similar results were reported from polycrystalline La$_{1-x}$Ca$_x$MnO$_3$ (Ref. 11) and oxygen-doped ceramic LaMnO$_{3+\delta}$.[13] Moreover, the single crystals exhibit a pronounced anisotropy of the resonance linewidth in the Jahn-Teller distorted phase, which disappears at temperatures $T > T_{JT}$. The pure LaMnO$_3$ sample turned out to be strongly twinned and, therefore, did not allow a detailed analysis of the angular dependence. Instead, the La$_{0.95}$Sr$_{0.05}$MnO$_3$ crystal was found to be untwinned and can effectively be treated like the mother compound ($x=0$), as it is still an antiferro-

magnetic insulator ($T_N = 140$ K) showing a similar magnetic susceptibility. Only the JT transition is shifted to lower temperatures, with $T_{JT}(x=0.05) = 600$ K.

In an earlier approach,[10] we ascribed the orientation dependence of the ESR linewidth to the influence of the Dzyaloshinsky-Moriya (DM) interaction, which arises from the tilting of the MnO$_6$ octahedra along the antiferromagnetically coupled b axis, only. However, the orthorhombic distortion of the MnO$_6$ octahedra itself gives rise to a crystal-field- (CF) induced line broadening of comparable order of magnitude[11,12] and for a complete description one has also to take into account the DM interaction via Mn-O-Mn bonds within the ferromagnetically coupled ac plane, which is smaller than along the b axis but not negligible.

In the present paper, we analyze the full angular dependence of the resonance field and linewidth for the three main crystallographic planes in the paramagnetic regime of the JT distorted phase and extract the microscopic CF parameters D and E and the DM vectors for all Mn-Mn pairs. For experimental details and evaluation of the ESR spectra we refer to our previous publication.[10] Our analysis is based on the structural data for LaMnO$_3$ determined from neutron-scattering experiments by Huang *et al.*[14] Throughout this paper we will use the crystallographic notation following Huang *et al.*, where the b axis (instead of the former c axis in Ref. 10) denotes the direction perpendicular to the ferromagnetically coupled ac planes.

II. THEORETICAL BACKGROUND

A strongly exchange-coupled magnetic system such as LaMnO$_3$ can be described by the following Hamiltonian:

$$\mathcal{H} = J \sum_{(i<j)} \mathbf{S}_i \cdot \mathbf{S}_j - \mu_B \sum_i \mathbf{H} \cdot \mathbf{g} \cdot \mathbf{S}_i + \mathcal{H}_{int}, \quad (1)$$

where the first term describes the superexchange interaction between two next-neighbor Mn spins $\mathbf{S}_i$ and $\mathbf{S}_j$ with coupling

constant J. The second term describes the Zeeman splitting of the spin states with gyromagnetic tensor **g** within an external magnetic field **H**. The third term $\mathcal{H}_{\text{int}}$ includes all interactions, which do not conserve the total spin and, therefore, contribute to the broadening of the ESR line. These are the CF, DM, anisotropic exchange (AE), dipole-dipole, and hyperfine interactions. An estimation of their relative strength[11] shows that CF and DM interactions yield by far the largest contribution.

To derive the appropriate expressions for CF and DM interaction, we use the structural parameters of the LaMnO$_3$-IIa sample (space group $Pnma$) determined by Huang *et al.*,[14] because it shows an antiferromagnetic ground state and an ordering temperature of about 140 K, which is consistent with the magnetic properties of our sample.[15] Figure 7(a) in Ref. 14 shows the crystallographic structure of LaMnO$_3$ in the strongly Jahn-Teller distorted phase. The long axes of the MnO$_6$ octahedra are found close to the ac plane and are rotated with respect to their next neighbors within the ac plane by about 90°. Additional tilting along the b axis gives rise to four inequivalent positions of manganese ions in the orthorhombic unit cell, which is illustrated in Fig. 7(b) of the same Ref. 14.

In a local coordinate system (ξ, η, ζ), where the axes are directed along the Mn-O bonds of the MnO$_6$ octahedra, the spin Hamiltonian of the crystal field can be written in terms of cartesian spin components (S_ξ, S_η, S_ζ) with parameters D and E as[16]

$$\mathcal{H}^{\text{CF}} = D' S_\zeta^2 + E' S_\eta^2, \tag{2}$$

where $D' = D - E$ and $E' = -2E$. The ζ axis is directed along the longest Mn-O bond close to the ac plane and the η axis is parallel to the Mn-O(1) bond almost along the b direction. Small orthorhombic distortions of the MnO$_6$ octahedron will be neglected here. Transformation into the crystallographic system (x,y,z along a,b,c axes) yields the matrix elements $D_{\alpha\beta}^{(j)}$, where $(\alpha,\beta) = (x,y,z)$ and $j = 1, \ldots, 4$ runs over the four nonequivalent Mn places.

The Hamiltonian, which describes the antisymmetric DM interaction,[17] can be written as

$$\mathcal{H}_{\text{DM}} = \mathbf{G}_{ij} \cdot [\mathbf{S}_i \times \mathbf{S}_j], \tag{3}$$

with the DM vector $\mathbf{G}_{ij} = d_{ij} \cdot [\mathbf{n}_{Oi} \times \mathbf{n}_{Oj}]$ being perpendicular to the plane defined by a Mn ion at site i, the bridge ligand O, and a Mn ion at site j, where **n** are unit vectors along Mn^{3+}-O^{2-} bonds.[18,19] The intrinsic scalar parameter d_{ij} strongly depends on the orbital states and the Mn-O-Mn bridge angle. In the case of pure LaMnO$_3$ both the tilting and the JT distortion of the MnO$_6$ octahedra account for the origin of antisymmetric contributions to the superexchange interaction between the Mn ions. A necessary condition for the existence of DM contributions is the lack of a center of inversion between the magnetic ions.[17] With the apical oxygen being shifted away from the [010] axis, there is a rather strong DM coupling between the ac planes and a smaller coupling within the ac planes. Figure 1 depicts all next-neighbor couplings that give rise to a DM interaction.
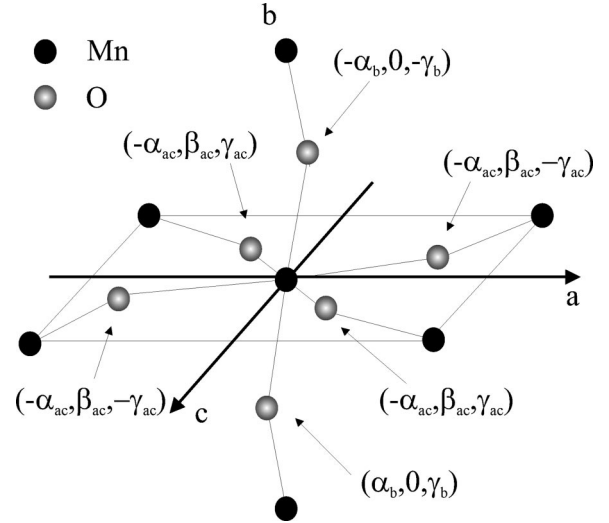

FIG. 1. Next-neighbor bonds of the Mn ions. α, β, and γ denote the cartesian components of the DM vector $\mathbf{G}_{ij}$.

For the $Pnma$ structure, the components G_{ij}^α ($\alpha = x,y,z$) of the DM vectors of all Mn pairs within the unit cell can be easily obtained and the absolute values can then be expressed via two parameters d_1 (inter-ac plane) and d_2 (intra-ac plane).

In the case of strong exchange narrowing ($\mathcal{H}_{\text{ex}} \gg \mathcal{H}_{\text{int}}$), the ESR linewidth ΔH is determined by the second moment M_2 of the resonance line divided by the exchange frequency ω_{ex},[20]

$$\Delta H \simeq \frac{\hbar}{g\mu_B} \frac{M_2}{\omega_{\text{ex}}}. \tag{4}$$

In the present case the second moment is determined by the sum of DM and CF contributions ($M_2^{\text{DM}} + M_2^{\text{CF}}$).

Within the coordinate system, where the z axis is determined by the external magnetic field, the second moment due to the Dzyaloshinsky-Moriya interaction is calculated as[21,22]

$$M_2^{\text{DM}} = \frac{2}{3} S(S+1) \sum_{i,j} [(\tilde{G}_{ij}^x)^2 + (\tilde{G}_{ij}^y)^2 + 2(\tilde{G}_{ij}^z)^2]. \tag{5}$$

The index $j = 1, \ldots, 4$ is running over all four magnetically inequivalent positions of the Mn ion in the unit cell. The sum over index $i = 1, \ldots, 6$ refers to the six next Mn neighbors around each Mn site with number j. After transformation into the crystallographic system, the average over all four positions yields the angular dependence

$$M_2^{\text{DM}} = \tfrac{2}{3} S(S+1) \{ (2\alpha_b^2 + 4\alpha_{ab}^2)[1 + \sin^2\theta \cos^2\varphi] + 4\beta_{ab}^2 [1$$
$$+ \sin^2\theta \sin^2\varphi] + (2\gamma_b^2 + 4\gamma_{ab}^2)[1 + \cos^2\theta]\}. \tag{6}$$

Polar angle θ and azimuth angle φ are measured with respect to the c and a axes of the orthorhombic unit cell.

For the crystal field, the expression for the second moment in the crystallographic system reads, e.g., for the ab plane

$$M_2^{CF}(ab) = \frac{1}{80}[4S(S+1)-3]\left\{\frac{1}{2}\sum_j [2D_{zz}^{(j)}-D_{xx}^{(j)}-D_{yy}^{(j)}]^2\right.$$

$$+\frac{5}{2}\sum_j [(D_{xx}^{(j)}-D_{yy}^{(j)})^2+4(D_{xy}^{(j)})^2]$$

$$+7\sum_j [(D_{zy}^{(j)})^2+(D_{xz}^{(j)})^2]+\sum_j [3(D_{zy}^{(j)})^2$$

$$-3(D_{xz}^{(j)})^2-(2D_{zz}^{(j)}-D_{xx}^{(j)}-D_{yy}^{(j)})$$

$$\left.\times(D_{xx}^{(j)}-D_{yy}^{(j)})]\cos 2\varphi\right\}. \tag{7}$$

The respective expressions for the ac and bc planes are obtained by the permutation of (x,y,z) and exchange of $\varphi \to \theta$. Again, the sum over j is running over the four inequivalent Mn positions in the unit cell.

The resonance field of the strongly exchange-narrowed ESR line is analogously determined by the first moment of the spectrum. Here we assume an isotropic g value, because the influence of the AE interaction can be neglected with respect to the crystal field.

The DM interaction does not contribute to the resonance shift, because its first moment vanishes. Hence, the resonance shift is determined by the crystal field alone, and the straightforward calculation yields the ESR frequency ν,

$$(h\nu)^2 = \left[g\mu_B H + \frac{M_{at}}{4g\mu_B}\sum_j (\tilde{D}_{xx}^{(j)}+\tilde{D}_{yy}^{(j)}-2\tilde{D}_{zz}^{(j)})\right]^2$$

$$-\frac{M_{at}}{4g\mu_B}^2\left[\sum_j (\tilde{D}_{xx}^{(j)}-\tilde{D}_{yy}^{(j)}+2i\tilde{D}_{xy}^{(j)})\right]$$

$$\times\left[\sum_j (\tilde{D}_{xx}^{(j)}-\tilde{D}_{yy}^{(j)}-2i\tilde{D}_{xy}^{(j)})\right]. \tag{8}$$

Here $M_{at}=(g\mu_B)^2 S(S+1)H/[3k(T-\Theta_{CW})]$ is the magnetization per Mn site and $\Theta_{CW}=111$ K is the paramagnetic Curie-Weiss temperature. The crystal-field components $\tilde{D}_{\alpha\beta}$ refer to the coordinate system in which the external field determines the z axis and are related to the components $D_{\alpha\beta}$ in the crystallographic system via the usual transformation rules. The sum over j is running over the four inequivalent Mn positions of the unit cell. The angular dependence of the resonance field $H_{res}(\theta,\varphi)$ is obtained after substitution of $\tilde{D}_{\alpha\beta}$ by $D_{\alpha\beta}$. For the interested reader a more detailed derivation of the above results can be found in Ref. 23.

Note that we also analyzed the effect of an anisotropy of the g factors. As a rule they are slightly different: $g_{zz} \neq g_{xx}, g_{yy}$.[16] This anisotropy also produces an effect in the angular dependence of the linewidth and the resonance field. For Mn^{3+} and Mn^{4+}, however, this anisotropy is usually smaller than $(g_\parallel - g_\perp)/g < 0.5\%$, even in the presence of a crystal field of the order of $D=1$ K.[24] This g-factor anisotropy results in a field anisotropy with an amplitude smaller than 20 Oe, which is about 10% of the effect observed at 200
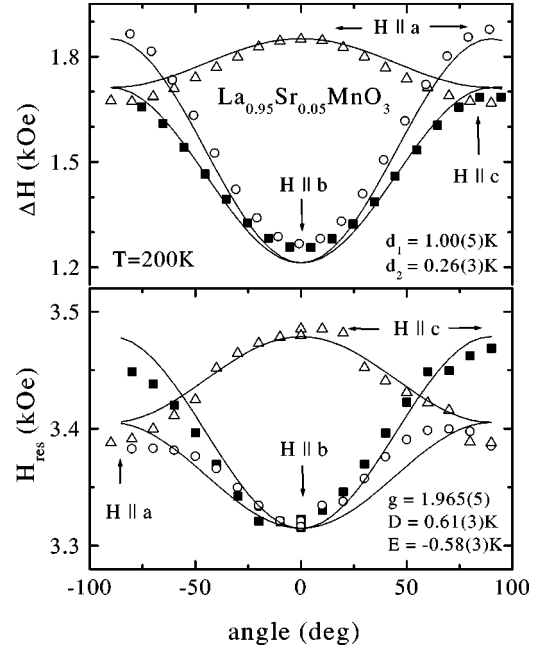

FIG. 2. Angular dependence of the ESR linewidth ΔH (upper frame) and resonance field H_{res} (lower frame) in $La_{0.95}Sr_{0.05}MnO_3$ for the magnetic field applied within the three crystallographic planes at 200 K. The solid lines represent the fit with Eqs. (4) and (8), respectively.

K. Concerning the anisotropy of the linewidth it accounts for only about 0.01% of what we observe experimentally.

III. DATA ANALYSIS AND DISCUSSION

As is shown in Fig. 2, at 200 K the resonance field and linewidth data can simultaneously be fitted for the three crystallographic planes by the contributions of CF and DM interactions only, without any additional parameters such as, e.g., a residual linewidth.

The superexchange integral J was estimated in mean-field approximation from the Curie-Weiss temperature $\Theta_{CW} = C(4J_{ac}+2J_b)$ with ferromagnetic in-plane coupling J_{ac} to four neighboring Mn ions and antiferromagnetic interplane coupling J_b to two neighboring Mn ions and the Curie constant $C=S(S+1)/3k_B$ (k_B is the Boltzmann constant). Assuming $-J_{ac}=J_b=J$ and inserting $S=2$ (Mn^{3+}) and $\Theta_{CW}=111$ K,[15] we obtain $J=14$ K. Both DM and CF interactions are of equal order of magnitude, about 1 K. The DM interaction, $d_1=1.00(5)$ K, along the antiferromagnetically coupled b axis is about four times larger than $d_2=0.26(3)$ K within the ferromagnetically coupled ac plane. The absolute values of the crystal-field parameters $D=0.61(3)$ K and $E=-0.58(3)$ K are of nearly equal strength indicating comparable axial (D) and rhombic (E) distortions of the MnO_6 octahedra.

The angular dependence of the resonance linewidth at 300 K is well fitted with similar but slightly larger parameters [$d_1=1.00(5)$ K, $d_1=0.30(3)$ K, $D=0.73(3)$ K, $E=-0.63(3)$ K] in Fig. 3, where we additionally visualized the angular dependence of both DM and CF contributions.
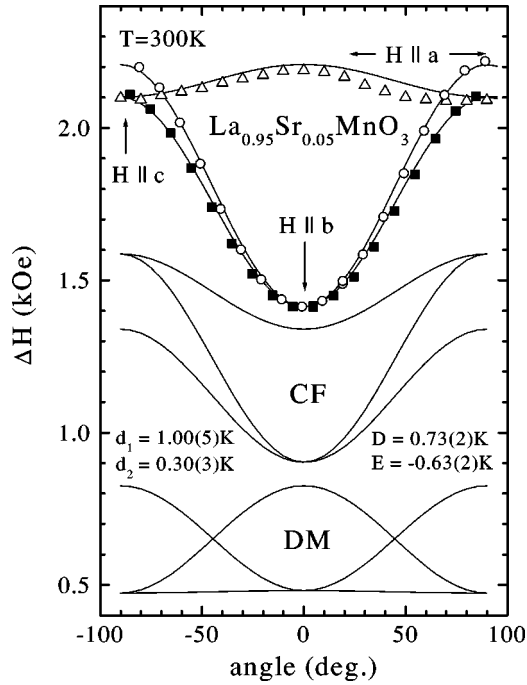
FIG. 3. Angular dependence of the ESR linewidth ΔH in $La_{0.95}Sr_{0.05}MnO_3$ for the magnetic field applied within the three crystallographic planes at 300 K. The solid lines represent the fit with Eq. (4). The lines below illustrate the contributions of CF and DM interactions, respectively.

The angular dependence of the resonance field at 300 K (not shown in Fig. 3) varies within the field range $3380 < H_{res} < 3480$ Oe, but suffers strongly from the onset of the skin effect due to the higher conductivity as compared to 200 K.[10] The skin effect produces an additional asymmetry of the ESR spectrum, which depends on the orientation and shape of the sample. In the case of large linewidths, the resonance field and asymmetry parameter exhibit a strong feedback on each other, which allows to fit the same spectrum by different sets of parameters. Only the linewidth remains stable. Within the ab and bc planes the change of asymmetry is directly correlated with an additional modulation of the resonance field. This is already slightly visible in the resonance field data at 200 K but becomes quite dominant at 300 K, and hence makes a description with Eq. (8) impossible.

As the derivation of the linewidth was carried out in the high-temperature limit ($T \gg \Theta_{CW}$), where it approximates an asymptotic value $\Delta H(\infty)$, we have to take into account that the fit parameters D, E, d_1, and d_2 should reflect the temperature dependence. According to Huber *et al.*[11] far apart from any magnetic or structural transitions, the temperature dependence can be approximated by the quotient of the single-ion Curie susceptibility and the experimental Curie-Weiss susceptibility as

$$\Delta H(T) = \frac{T - \Theta_{CW}}{T} \Delta H(\infty). \qquad (9)$$

Taking into account that the square of CF and DM parameters appears in the formulas for the second moment, we can extrapolate these parameters for $T \to \infty$ via the square root of Eq. (9). Using the data at 300 K, which is far above magnetic order, we have to multiply the parameters by a factor of 1.26 and get $D(\infty) = 0.91$ K, $E(\infty) = -0.79$ K, $d_1(\infty) = 1.26$ K, and $d_2(\infty) = 0.38$ K. Comparing the values at 200 K, one expects a reduction of the parameters by approximately 15% with respect to 300 K. Indeed, this is well fulfilled, despite the onset of the critical behavior on approaching magnetic order at 140 K; only d_1 remains unchanged.

The equations for the resonance field already contain the temperature dependence within the magnetization $M(T)$. For this reason it would be better described by the high-temperature values of the CF parameters than by the temperature-dependent ones, which is the case at 200 K. Due to the rather large uncertainty in the determination of the resonance field and the proximity of the critical temperature region, this discrepancy is not assumed to be of significant importance. Thus, at 300 K the amplitude of the uncorrected resonance-field anisotropy is nicely reproduced by the high-temperature values of the CF parameters as $H_{res}^{max} - H_{res}^{min} = 95$ Oe.

The strength of CF and DM interaction was independently determined from orientation-dependent magnetization data,[25] measured at 4.2 K in a $La_{0.95}Sr_{0.05}MnO_3$ single crystal of the same batch as used in our ESR experiments. In combination with antiferromagnetic-resonance measurements, it was shown there that the ground state ($T < T_N$) exhibits a canted antiferromagnetic structure, which rules out any phase separation in ferromagnetic and antiferromagnetic regions. Within the two-sublattice model Pimenov *et al.* obtained (after translation to our Hamiltonian in units of K) the following parameters from the magnetization data:[25] $J = 13.2$ K, $K_z = -2E = 0.93$ K, $K_x = D - E = 0.95$ K, and $G = \sin(155°)d_1 = 1.18$ K. These results are in good agreement with our findings, as the values of the CF parameters $D = 0.48$ K and $E = -0.47$ K are essentially equal. The DM contribution is of similar strength, where d_2 was neglected. Thus, we could confirm the validity of their model from a microscopic point of view.

ESR studies by Huber *et al.*[11] in $LaMnO_3$ and Tovar *et al.*[13] in the series $LaMnO_{3+\delta}$ revealed values comparable to our parameters. For pure $LaMnO_3$, they used the CF parameter $D = 1.92$ K determined by Moussa *et al.* from neutron-scattering experiments[26] and estimate the DM contribution as $d \approx 0.8$ K. For an oxygen excess $\delta = 0.03$ with a transition temperature $T_{JT} = 600$ K comparable to $La_{0.95}Sr_{0.05}MnO_3$, the CF parameter D is found to be about 20% smaller than in the pure compound, whereas the DM interaction remains essentially unchanged at $d \approx 0.8$ K. Though these data were measured in polycrystalline samples, where no distinction between axial (D) and rhombic (E) CF parameters and the interplane and intraplane DM interaction could be made, their results agree with ours within a factor of 2.

The fact that the two CF parameters are of comparable

strength is of particular importance for the picture of orbital order in $LaMnO_3$. Considering the equal contributions of D and E, we conclude that the simple picture of ordering of $d_{3z^2-r^2}$ orbitals has to be modified as it results in $E=0$, in contradiction to our findings. In a local coordinate system the orbital of the e_g electron is a superposition $\psi_{g,e} = c_1\phi_{3z^2-r^2} \pm c_2\phi_{x^2-y^2}$,[27] where $c_1 \approx 0.8$ and $c_2 \approx 0.6$ denote the orbital mixing coefficients down to lowest temperatures as reported by Rodriguez-Carvajal *et al.*[7] on the base of neutron-diffraction studies. Matsumoto[27] found $E \propto -c_1c_2$ and $D \propto c_1^2 - c_2^2$ in second-order perturbation theory. This simple approach qualitatively confirms our results, as not only the sign of our parameters is reproduced but also both orbital-mixing coefficients must not be negligibly small in order to explain the observed rhombic CF parameter E. From the neutron-diffraction data one can estimate from $\tan \theta/2 = c_2/c_1$ the orbital component as $\theta = 106°$ in comparison to $\theta = -59°$ and $-56°$, estimated by using $E/D = 1/\sqrt{3} \tan \theta$ (Ref. 16) from our results at 200 K and 300 K, respectively.

Very recently Tobe *et al.*[28] reported a discrepancy between the anisotropy of the optical spectra in pure $LaMnO_3$ and the orbital component of $\theta \sim 108°$ as determined from c_1 and c_2 by neutron scattering. The authors explain this deviation within a simple p-d transition model using an additional d-d character of the transition. Considering our value of $\theta \sim -60°$, their model gives a ratio of $I_c/I_{ab} = 0.4$ instead of 1.2 for $\theta \sim 108°$. Thus, we conclude that one can explain their experimental ratio of 0.6 without invoking a d-d character and, therefore, a value of $\theta \sim -60°$ holds for a more consistent picture of the properties of $LaMnO_3$.

IV. CONCLUSION

We have performed a systematic investigation of the angular dependence of the paramagnetic resonance in the Jahn-Teller distorted orthorhombic phase in $La_{0.95}Sr_{0.05}MnO_3$ single crystals. We have also presented a comprehensive analysis for the resonance linewidth in the high-temperature approximation, which takes into account the microscopic geometry of the four inequivalent Mn positions in the orthorhombic unit cell based on the structural data determined for $LaMnO_3$ by Huang *et al.*[14] The crystal-field parameters for all Mn positions and the Dzyaloshinsky-Moriya interaction for nearest-neighbor Mn ions along the b axis as well as in the ac plane were successfully extracted as $D(\infty) = 0.91$ K, $E(\infty) = -0.79$ K, $d_1(\infty) = 1.26$ K, and $d_2(\infty) = 0.38$ K. These findings shed new light on the microscopic picture of orbital order and the spin-spin interaction in these compounds.

[1] A.K. Bogush, V.I. Pavlov, and L.V. Balyko, Cryst. Res. Technol. **18**, 589 (1983); M. Paraskevopoulos, F. Mayr, C. Hartinger, A. Pimenov, J. Hemberger, P. Lunkenheimer, A. Loidl, A.A. Mukhin, V.Yu. Ivanov, and A.M. Balbashov, J. Magn. Magn. Mater. **211**, 118 (2000); A. Urushibara, Y. Moritomo, T. Arima, A. Asamitsu, G. Kido, and Y. Tokura, Phys. Rev. B **51**, 14 103 (1995); J.-S. Zhou, J.B. Goodenough, A. Asamitsu, and Y. Tokura, Phys. Rev. Lett. **79**, 3234 (1997).

[2] D.I. Khomskii, Int. J. Mod. Phys. B **15**, 2665 (2001).

[3] Myron B. Salomon and Marcelo Jaime, Rev. Mod. Phys. **77**, 583 (2001).

[4] E. Dagotto, T. Hotta, and A. Moreo, Phys. Rep. **344**, 1 (2001).

[5] J.B. Goodenough, A. Wold, R.J. Arnott, and N. Menyuk, Phys. Rev. **124**, 373 (1961).

[6] Y. Murakami, J.P. Hill, D. Gibbs, M. Blume, I. Koyama, M. Tanaka, H. Kawata, T. Arima, Y. Tokura, K. Hirota, and Y. Endoh, Phys. Rev. Lett. **81**, 582 (1998).

[7] J. Rodriguez-Carvajal, M. Hennion, F. Moussa, A.H. Moudden, L. Pinsard, and A. Revcolevschi, Phys. Rev. B **57**, R3189 (1998).

[8] E. Saitoh, S. Okamoto, K.T. Takahashi, K. Tobe, K. Yamamoto, T. Kimura, S. Ishihara, S. Maekawa, and Y. Tokura, Nature (London) **410**, 180 (2001).

[9] E. Granado, N.O. Moreno, A. Garcia, J.A. Sanjurjo, C. Rettori, I. Torriani, S.B. Oseroff, J.J. Neumeier, K.J. McClellan, S.-W. Cheong, and Y. Tokura, Phys. Rev. B **58**, 11 435 (1998).

[10] V.A. Ivanshin, J. Deisenhofer, H.-A. Krug von Nidda, A. Loidl, A.A. Mukhin, A.M. Balbashov, and M.V. Eremin, Phys. Rev. B **61**, 6213 (2000).

[11] D.L. Huber, G. Alejandro, A. Caneiro, M.T. Causa, F. Prado, M. Tovar, and S.B. Oseroff, Phys. Rev. B **60**, 12 155 (1999).

[12] B.I. Kochelaev (unpublished).

[13] M. Tovar, G. Alejandro, A. Butera, A. Caneiro, M.T. Causa, F. Prado, and R.D. Sánchez, Phys. Rev. B **60**, 10 199 (1999).

[14] Q. Huang, A. Santoro, J.W. Lynn, R.W. Erwin, J.A. Borchers, J.L. Peng, and R.L. Greene, Phys. Rev. B **55**, 14 987 (1997).

[15] M. Paraskevopoulos, F. Mayr, J. Hemberger, A. Loidl, R. Heichele, D. Maurer, V. Müller, A.M. Mukhin, and A.M. Balbashov, J. Phys.: Condens. Matter **12**, 3993 (2000).

[16] A. Abragam and B. Bleaney, *EPR of Transition Ions* (Clarendon Press, Oxford, 1970).

[17] T. Moriya, Phys. Rev. Lett. **4**, 228 (1960); Phys. Rev. **120**, 91 (1960).

[18] F. Keffer, Phys. Rev. **126**, 896 (1962).

[19] A.S. Moskvin and I.G. Bostrem, Fiz. Tverd. Tela (Leningrad) **19**, 2616 (1977) [Sov. Phys. Solid State **19**, 1532 (1977)].

[20] P.W. Anderson and P.R. Weiss, Rev. Mod. Phys. **25**, 269 (1953).

[21] T.G. Castner, Jr. and M.S. Seehra, Phys. Rev. B **4**, 38 (1971).

[22] Z.G. Soos, K.T. McGregor, T.T.P. Cheung, and A.J. Silverstein, Phys. Rev. B **16**, 3036 (1977).

[23] J. Deisenhofer, M. Eremin, D.V. Zakharov, V.A. Ivanshin, R.M. Eremina, H.-A. Krug von Nidda, A.A. Mukhin, A.M. Balbashov, and A. Loidl, cond-mat/0108515 (unpublished).

[24] S. A. Alt'shuler and B. M. Kozyrev, *Electron Paramagnetic Resonance* (Nauka, Moscow, 1972).

[25] A. Pimenov, M. Biberacher, D. Ivannikov, A. Loidl, V.Yu. Ivanov, A.A. Mukhin, and A.M. Balbashov, Phys. Rev. B **62**, 5685 (2000).

[26] F. Moussa, M. Hennion, J. Rodriguez-Carvajal, H. Moudden, L. Pinsard, and A. Revcolevschi, Phys. Rev. B **54**, 15 149 (1996).

[27] G. Matsumoto, J. Phys. Soc. Jpn. **29**, 606 (1970).

[28] K. Tobe, T. Kimura, Y. Okimoto, and Y. Tokura, Phys. Rev. B **64**, 184 421 (2001).